Interfacial Adhesion of Plasma-Treated Carbon Fiber/ Poly(phthalazinone ether sulfone ketone) Composite

Chun Lu,[1,2] Ping Chen,[1] Qi Yu,[2] Zhenfeng Ding,[3] Zaiwen Lin,[4] Wei Li[2]

[1]*State Key Laboratory of Materials Modification by Beams, School of Chemical Engineering, Dalian University of Technology, Dalian, Liaoning, China 116012*
[2]*Center for Composite Materials, Shenyang Institute of Aeronautical Engineering, Shenyang, Liaoning, China 110034*
[3]*State Key Laboratory of Materials Modification by Beams, Dalian University of Technology, Dalian, Liaoning, China 116023*
[4]*Harbin FRP institute, Harbin, Heilongjiang, China, 150036*

Received 2 December 2006; accepted 6 May 2007
DOI 10.1002/app.26840
Published online 17 July 2007 in Wiley InterScience (www.interscience.wiley.com).

ABSTRACT: Interfacial adhesion between fiber and matrix has a strong influence on composite mechanical performance. To exploit the reinforcement potential of the fibers in advance composite, it is necessary to reach a deeper understanding on the relation between fiber surface treatment and interfacial adhesion. In this study, air plasma was applied to modify carbon fiber (CF) surface, and the capability of plasma grafting for improving the interfacial adhesion in CF/thermoplastic composite was discussed and also the mechanism for composite interfacial adhesion was analyzed. Results indicated that air plasma treatment was capable of increasing surface roughness as well as introducing surface polar groups onto CF; both chemical bonding and mechanical interaction were efficient in enhancements of interlaminate shear strength of CF/PPESK composite, while mechanical interaction has a dominant effect on composite interfacial adhesion than chemical bonding interaction. © 2007 Wiley Periodicals, Inc. J Appl Polym Sci 106: 1733–1741, 2007

Key words: carbon fiber; poly(phthalazione ether sulfone keton) (PPESK); interface; plasma; XPS

INTRODUCTION

The application of carbon fiber (CF)/thermoplastic composites has continuously risen during the last decade, especially in car and aerospace industries, because of the improvement of the damage tolerance and mechanical stiffness.[1–6] The mechanical property of fiber-reinforced composites depends mainly on the properties of the fiber and on the degree of adhesion between the fiber and the matrix. However, untreated carbon fibers (CF) have smooth and inert surface; therefore, are unable to form strong interaction between their surfaces and the matrix. Various techniques have been developed for CF surface treatment, such as sizing, HNO_3 oxidation, electrochemical oxidation, and plasma treatment. Among these applications, plasma treatment is an effective method in increasing CF polarity as well as surface roughness, which will improve composite interfacial adhesion by chemical and mechanical interaction between CF and matrix.[7–15]

Correspondence to: P. Chen (chenping_898@126.com).
Contract grant sponsor: Natural Science Foundation of Liaoning Province; contract grant number: 20044002.

Poly(phthalazinone ether sulfone ketone) (PPESK) is a kind of novel thermoplastic with excellent mechanical properties, remarkable thermal and chemical resistance. CF/PPESK composite can be used in aerospace, automobile, and sporting goods industries. However, because of the chemical inertness and low surface free energy of the CF, interfacial adhesion between fiber and matrix is weak, and the performance of CF/PPESK composite is restricted. The aim of this paper is to study the plasma-treated CF surface characteristics and their behavior in CF/PPESK composites. The extent of surface modification was evaluated by X-ray photoelectron spectroscopy (XPS) analyze, AFM, and fiber surface free energy, composite interfacial properties were characterized by interfacial shear strength and SEM.

EXPERIMENTAL

Materials

The matrix used is poly(phthalazione ether sulfone ketone) (characteristic viscosity (η): 0.35, glass transition temperature (T_g): 287°C. Dalian Polymer new material Co.).[16–21] The structure is shown in Figure 1.

From Figure 1 we can see that PPESK molecular is composed of rigid benzene and 4-(4′-hydroxy-

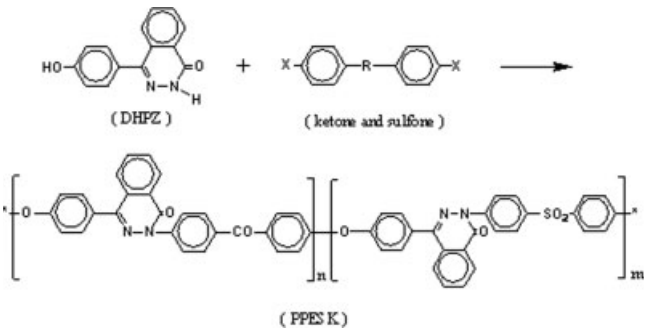

Figure 1 Structure of PPESK molecule.

phenyl)-2,3-phthalazin-1-one (DHPZ), linked together by ether-bond and polar groups of ketone and sulfone. Since noncoplanar twisted aromatic structure DHPZ is introduced into the polymer backbone, the matrix is endued with novel thermal resistance property and excellent solubility, thus fibers reinforced PPESK composite can be prepared conveniently by solution impregnation technique.[22] Solvent: DMAc, solution concentration (20 wt %); CFs (PAN base, T700sc, Toray), fiber surface were treated with acetone for de-sizing.

Fiber surface treatment

CF was treated in inductively coupled plasma (ICP, indicated in Fig. 2), air (dehydrated with wikipedia (γ-Al_2O_3)) was used as a carrier gas with 60–80 cm^3/min, plasma treatment time was varied from 5 to 20 min, and plasma discharge power was fixed at 250 W.

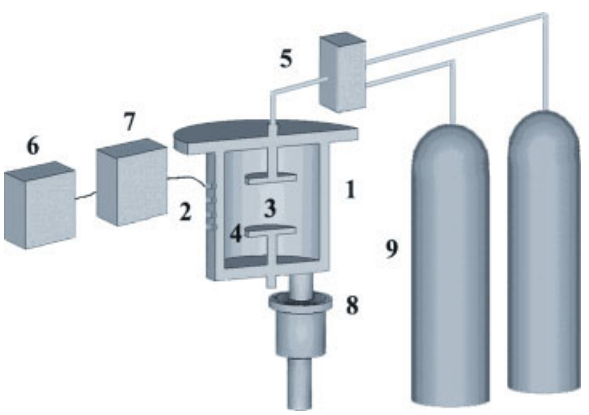

Figure 2 Sketch of Plasma instrument: 1, Pyrex glass tube; 2, Coil; 3, Reaction chamber; 4, Electrode; 5, Mass flow controller; 6, ICP power source; 7, Matching Box; 8, Molecular Pump; 9, Gas. [Color figure can be viewed in the online issue, which is available at www.interscience.wiley.com.]

Plasma treatment time: No. 1 : 0 min (CF-0 min); No. 2 : 5 min (CF-5 min); No. 3 : 10 min (CF-10 min); No. 4 : 15 min (CF-15 min); No. 5 : 20 min (CF-20 min).

Composite preparation and interfacial properties

Plasma grafting: after plasma treatment, CF was taken out from plasma reaction chamber and impregnated with the low viscosity PPESK/DMAc solution immediately, after removing the solvent (160°C/3 h, oven, 170°C/8 h vacuum oven), CF/PPESK composite was made by compression molding technique at 385°C.[4,23] The processing cycle is show in Figure 3.

Interlaminar Shear Strength of composites samples (dimensions 30 × 6 × 2 mm^3) were carried out using short-beam shear test (GB3357-82) on Shimadzu universal testing machine with a constant cross-head rate of 2 mm/min. interlaminate shear strength (ILSS) was calculated according to the equation as below:

$$\tau_s = \frac{3P_b}{4b \cdot h}$$

τ_s, ILSS; P_b, load at break; b, wide of the specimen; h, thickness of the specimen.

Morphologies of composite interlaminar shear ruptures were characterized using a JSM-5600LV scanning electron microscope (SEM), composites failure mechanisms were analyzed from the SEM pictures.

Fiber surface free energy

Fiber surface free energy was analyzed according to Wihelmy method, on a dynamic contact angle analy-

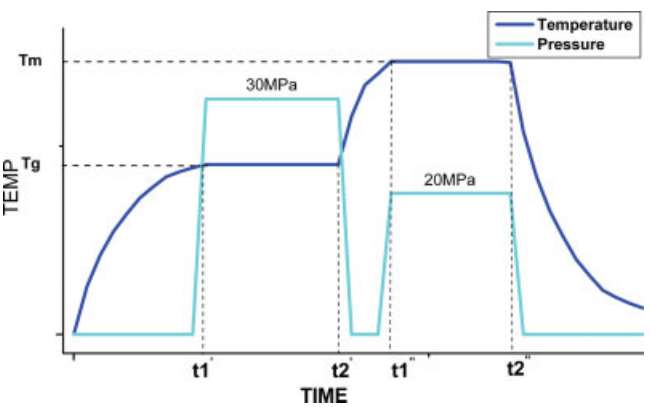

Figure 3 Composite processing cycle. [Color figure can be viewed in the online issue, which is available at www.interscience.wiley.com.]

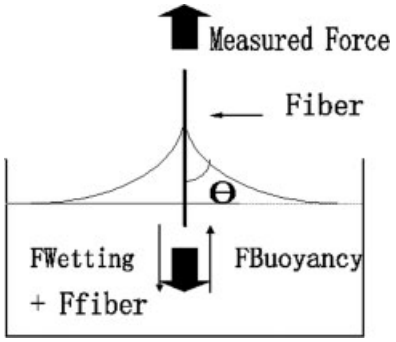

Figure 4 Sketch of dynamic contact angel measurement.

sis system (DCA-322, Thermo Cahn) (illustrated in Fig. 4)

$$F_{\text{Measured}} = F_{\text{Fiber}} - F_{\text{Buoyancy}} + F_{\text{Wetting}} \quad (1)$$

$$F_{\text{Wetting}} = \gamma \cdot p \cdot \cos\theta \quad (2)$$

$$\gamma = \gamma^p + \gamma^d \quad (3)$$

$$\gamma_l\,(1 + \cos\theta) = 2 \cdot \sqrt{\gamma_s^p \gamma_l^p} + 2 \cdot \sqrt{\gamma_s^d \gamma_l^d} \quad (4)$$

F_{Measured} is the total force exerted on the microbalance; F_{Fiber} is the gravitation of the fiber; F_{Buoyancy} is the buoyancy force of the fiber in the testing liquid; F_{wetting} is the wetting force between fiber and the testing liquid; P is the wetted perimeter; θ is the dynamic contact angle between fiber and liquid; γ is the surface tension of the testing liquid; γ^p is the polar component; γ^d is the dispersive component.

In experiment, a single fiber was mounted indirectly to a wire hook suspended from a microbalance and then immersed into the testing liquid by raising the elevating stage with the testing liquid reservoir. The force exerted on the fiber can be expressed as the sum of the wetting, gravitational, and buoyancy force, the measured force is given as eq. (1). By moving the stage up to a fixed immersion depth at a constant speed of 1 mm/min, a typical Force- high plot (y) was given schematically. Dynamic contact angles (θ) were calculated from eq. (2). Fiber surface free energy was calculated according to Owens-Wendt eqs. (3) and (4).[23–30]

Fiber surface chemical composition

Fiber surface chemical composition was analyzed by X-ray photoelectron spectroscopy (XPS) (Thermo, ESCALAB 250) using AlKa photo beams at normal emission angle. The element concentration on fiber surface was estimated according to the corresponding peak areas. The chemical states of the surface atoms of CFs were determined using non-Linear-Least-Squares-Curve fitting program with a Gaussian/Lorentzian production function.

Fiber surface topography

CF surface topography was characterized using a Solver P47 Atom0ic Force Microscopy (NT-MDT, Russia).

RESULT AND DISCUSSION

Influence of plasma treatment on CF surface composition

The surface chemical composition of the plasma-treated CF was characterized by XPS, and carbon, oxygen, and nitrogen contents were calculated according to the corresponding peak areas (Table I). As can be seen in Table I, oxygen concentration on the surface of CF was increased by plasma treatment from 17.4% of the untreated fiber to 18.8% of the 5 min treated case, and nitrogen concentration was increased from 0.16 to 1.28%. The increase of oxygen and nitrogen composition indicated that after plasma treatment, substantial amount of polar groups is introduced onto CF surface. We take a further analysis on fiber surface functional groups, and the results are shown in Figure 5.

For Figure 5(a) (Untreated CF), a single peak at 284.5 eV is due to —C—C— (H) group (content 71.1%), the peak at 285.7 eV might correspond to —C—N— (17.0%), the peak at 286.5 is considered to be —C—O— group (5.4%), and the peak at 289.3 eV might correspond to —COOH (or —COO—) group (6.5%), the ratio of polar/nonpolar is 0.41. After air plasma treated for 5 min [Fig. 6(b)], the content of polar component is 50.8%, and the ratio of polar/nonpolar is 1.03, the polarity of the fiber is increased significantly. The polar/nonpolar ratio changes little when plasma treatment time increases, and the ratio of polar/nonpolar remains at about 1.22. Results of C1s spectrum indicate a significant increase in —C—N—, —C—O—, —C=O, —COO— groups, which increase the polarity of the fiber surface. Besides, from Figure 5 we can see that plasma treatment increases CF surface polarity rapidly, after

TABLE I
Surface Chemical Composition of Fibers

	Chemical composition (%)		
Condition	C	O	N
Untreated	82.17	17.36	0.16
CF-5 min	79.90	18.82	1.28
CF-10 min	79.83	19.44	0.73
CF-15 min	80.40	18.69	0.90
CF-20 min	81.03	17.85	1.05

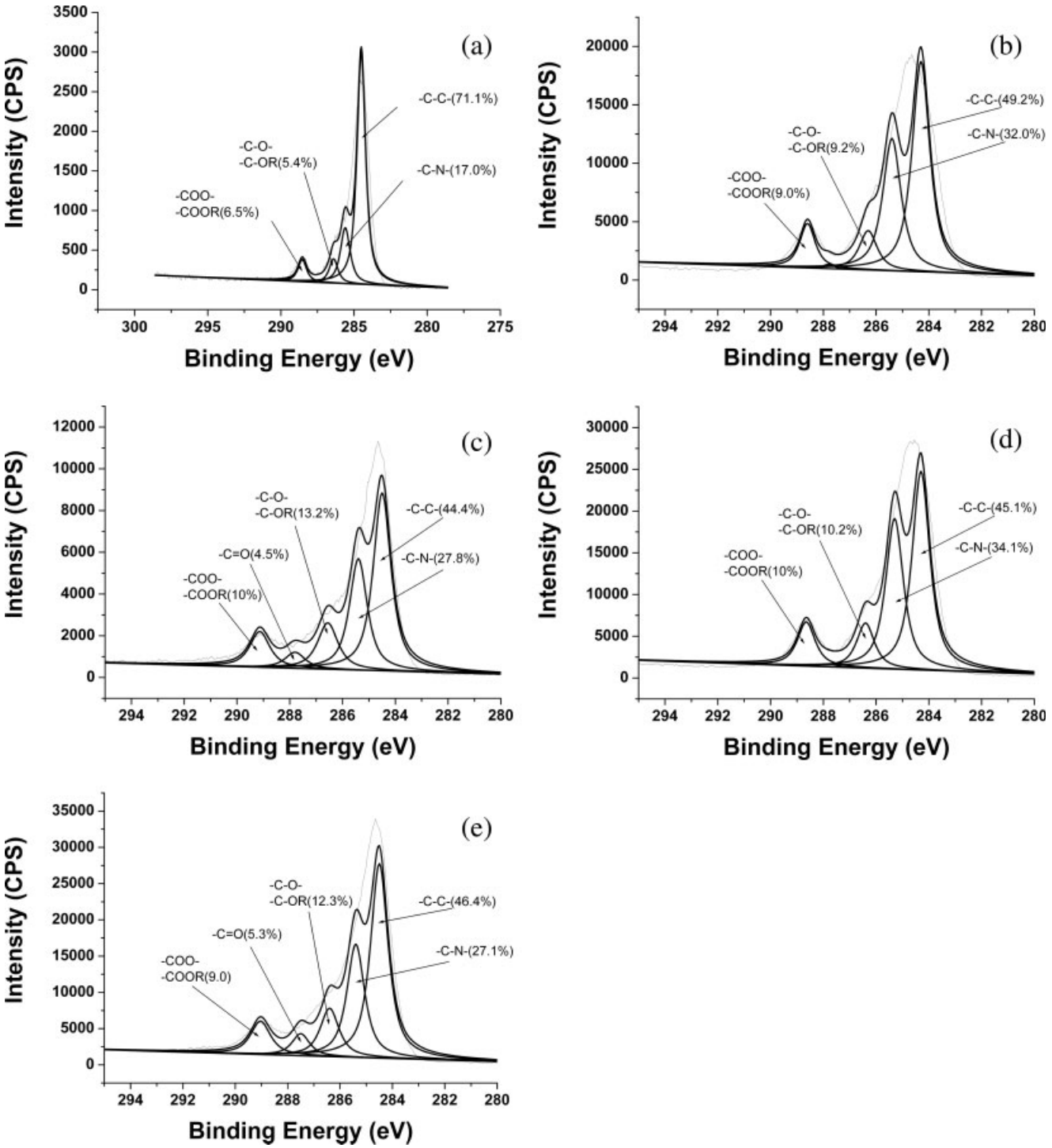

Figure 5 CF C1s with different plasma treating time. (a) CF-0 min; (b) CF-5 min; (c) CF-10 min; (d) CF-15 min; (e) CF-20 min.

being treated for 5 min, the content of CF polar groups have reached a high level.

Influence of plasma treatment on fiber surface roughness

Fiber surface topographies were indicated in Figure 6. From Figure 6(a) we can see that the surface of the untreated CF is smooth with little groves distributing along fiber surface. After being treated for 5 min [Fig. 6(b)], fiber surface was changed a little, a few shallow grooves distributing along the longitudinal direction of the fiber. However, after fiber being treated for more than 15 min [Fig. 6(c,d)], substantial amount of deep grooves can be seen on fiber surface, fiber surface roughness was changed dramatically.

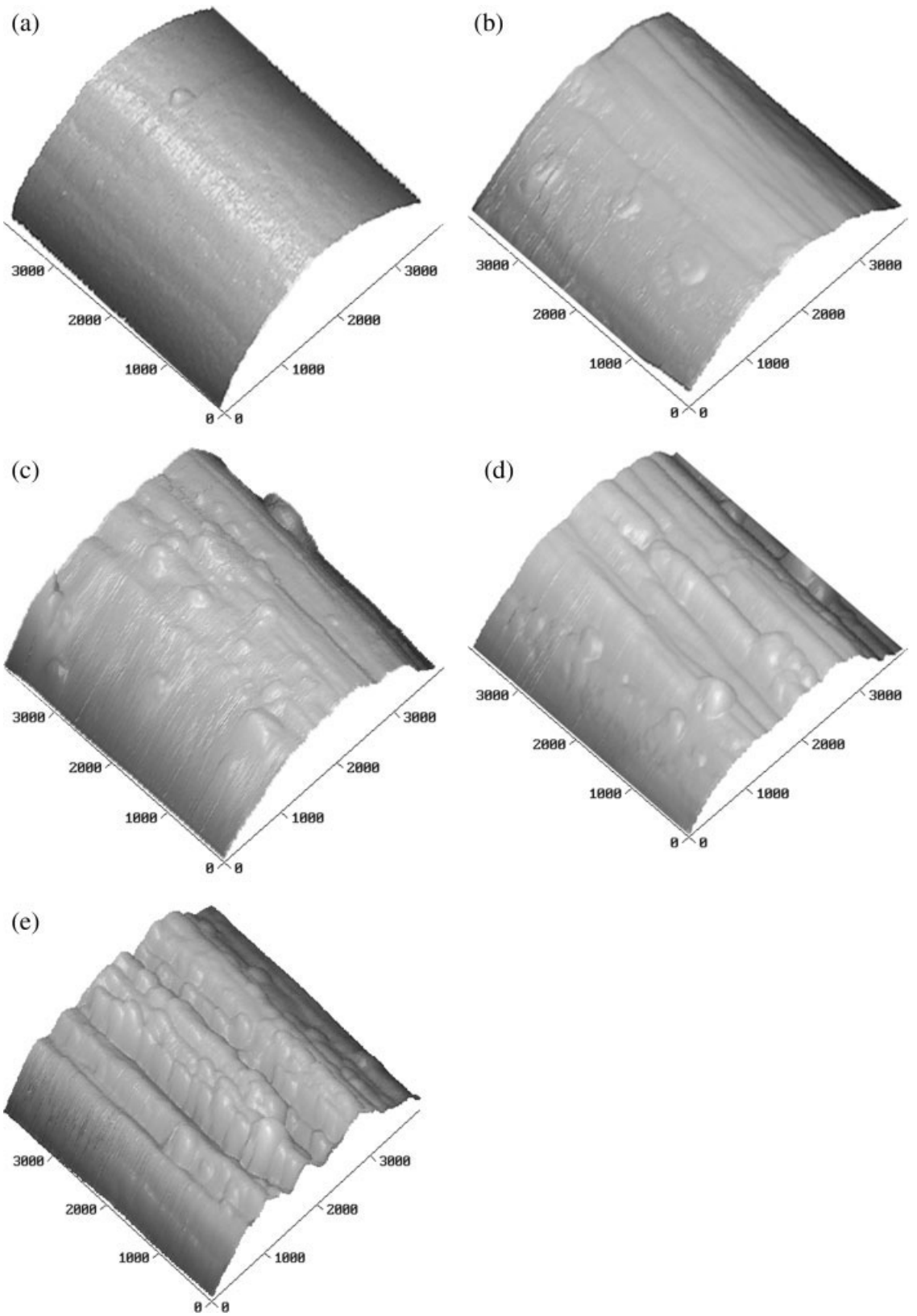

Figure 6 Topography of the CF surface (a) untreated; (b) plasma treated 5 min; (c) plasma treated 10 min; (d) plasma treated 15 min; (e) plasma treated 20 min.

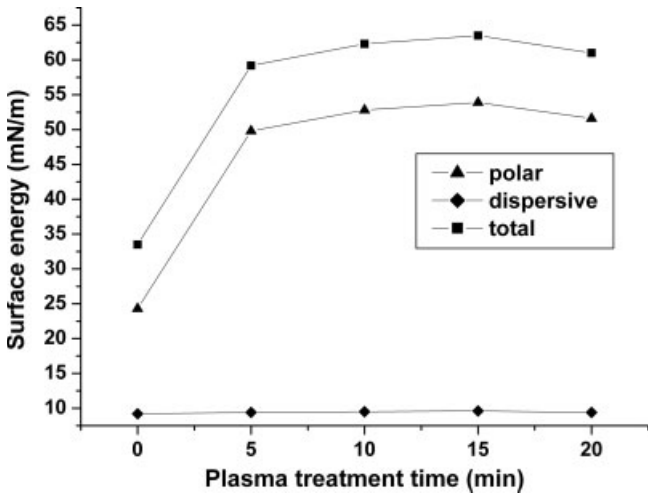

Figure 7 Surface free energies of plasma-treated CF.

Influence of plasma treatment on fiber wettability

The surface energies for the dispersive and polar components are summarized in Figure 7. The result indicates that the polar component and total energy increase steeply within the first 5 min, and then they level off to a saturation state of about 62.0 mN/m. There are little changes to the dispersive component.

The thermodynamic work of adhesion between fiber and solution (W_a) is given by the work required to separate reversibly the interface between two phases from their equilibrium to infinity. The energy balance is given by equation[26,30]:

$$W_a = 2\left[(\gamma_s^d \gamma_l^d)^{1/2} + (\gamma_s^p \gamma_l^p)^{1/2}\right] \quad (5)$$

From eq. (5) we can see that the thermodynamic work of adhesion (W_a) is determined by the surface free energy (γ) of fibers. When surface free energy is higher the work of adhesion is bigger, as a result, fibers can be well impregnated by solution. Surface free energy of untreated CF is 33.5 mN/m, after plasma treatment, CF surface free energy is 60.0 mN/m (mean value), the wettability of plasma-treated CF is better than that of untreated CF.

Influence of cold plasma treatment on composite interfacial adhesion

Composite ILSS is an effective method for indicating composite interfacial adhesion property. The ILSS of CF/PPESK composite is shown in Figure 8.

It can be seen from Figure 8 that the ILSS of CF/PPESK composite increases first and decreases afterwards with increasing plasma treatment time, and arrives at the maximum value at 15 min of plasma treatment. The ILSS of plasma-treated CF/PPESK composite was increased by 12.9% when compared with that of untreated CF/PPESK composite. However, after CF was treated for more than 15 min, composite ILSS shows a declining tendency. This probably due to excess plasma etching reduces the bulk performance of the fiber.[31] Besides, the increasing tendency of composite ILSS is similar to that of CF roughness, we will take a further discussion later.

Composite failure mechanism

When composite suffers from load, the stress distribution on the fiber and matrix satisfies the Kelly-Tyson theory.[1,24] On the basis of the theory, if a constant load loads on a nonfailing fiber fragment (with a diameter D and length L), the interfacial shear stress along the fiber is given by eq. (6):

$$\tau = \frac{D\sigma}{2L} \quad (6)$$

When interfacial adhesion is strong, destruction of the composite will take place in matrix near the interface, with resin adhesive on fiber surface. While interfacial adhesion is weak, fibers will be peeled off from matrix, the fiber is clean, with little resin adhesive on the surface.

From morphologies of composite interlaminar shear ruptures (Fig. 9), we can see that the ruptures of the composite with different treatments are obviously different. On the rupture of untreated CF composite [Fig. 9(a)], fibers are peeled off from the matrix, and the surface of the fibers are smooth

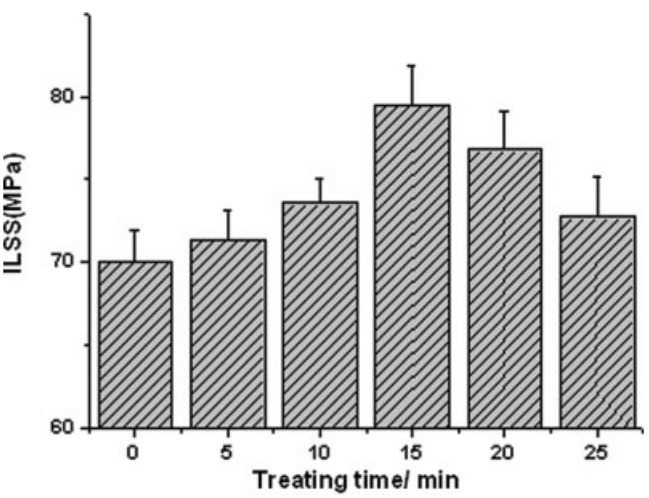

Figure 8 ILSS of CF/PPESK composite as a function of air plasma treating time.

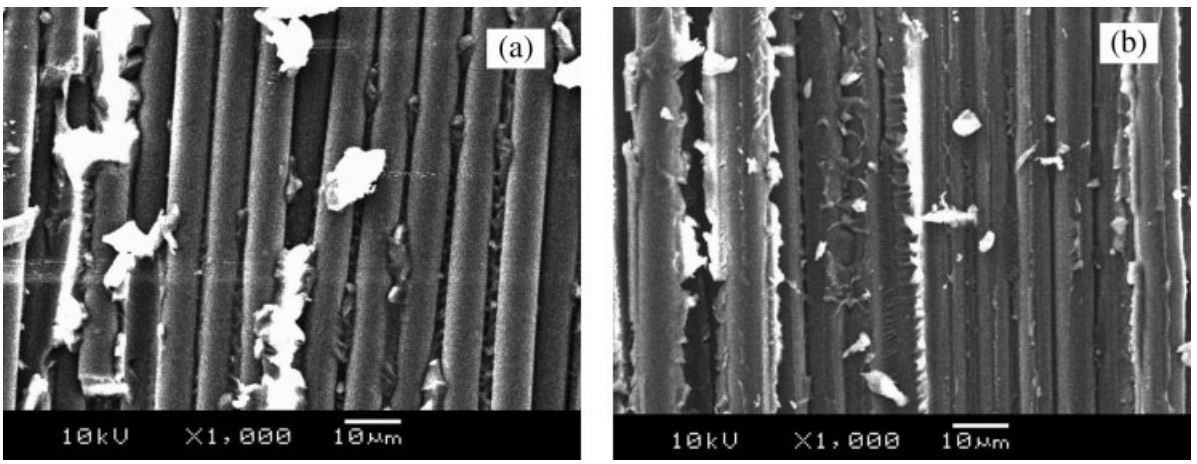

Figure 9 Morphology of interlaminar shear ruptures of the composites. (a) Untreated CF/PPESK composite; (b) plasma-treated CF/PPESK composite.

with a little resin adhesive on the surface, composite destruction takes place on interface between fiber and matrix. On the rupture of plasma-treated CF composite [Fig. 9(b)], considerable matrix deformation together with fibers are tightly held by the matrix. The primary failure mode in plasma-treated CF composites is matrix failure. As can be seen, after plasma treatment composite interfacial adhesion was improved significantly.

Composite interfacial adhesion mechanism

Researches indicate that at different plasma treatment stage, the mechanism of plasma surface treatment is different. Surface modification is dominant at the beginning, and then is overwhelmed by surface etching at a later stage of the process.[32,33] As a result of plasma treatment, CF surface polar groups increase more rapidly than fiber surface roughness.

In fiber/matrix composite, both chemical bonding and mechanical interaction have a positive effect on composite interfacial adhesion. Chemical bonding interaction is determined by the content of fiber surface polar group. From the analysis above, we can see that the content of fiber surface polar group increases rapidly within 5 min plasma treatment time. This indicated that CF surface chemical interaction may have been achieved at the early stage of

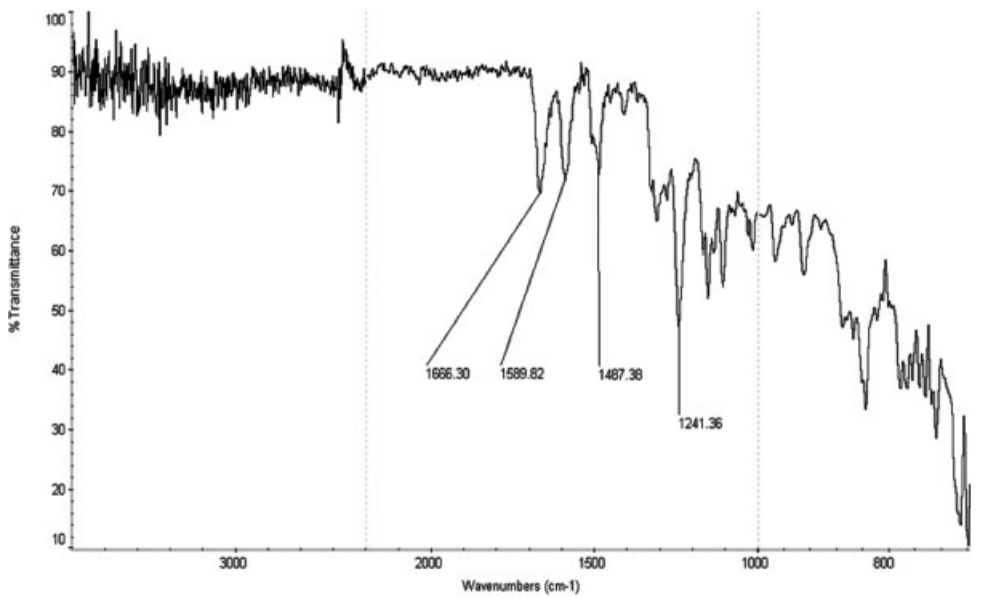

Figure 10 IR spectrum of plasma-grafted CF.

TABLE II
Surface Element Content (mol %) of the Untreated CF and Separated CF

Sample	C (282–289 eV)	O (528–536 eV)	N (396–402 eV)	S (168–172 eV)
Untreated CF	82.17	17.36	0.16	0
Separated CF	80.26	19.28	0.38	0.08

plasma treatment. To exploit the chemical interaction between plasma-treated CF and PPESK matrix, plasma-treated CF/PPESK composite were cut into smaller pieces, and immerged into sulfuric acid (98%) for 40 days. The resin on fiber surface was dissolved by the acid completely, only compounds which had strong interaction with the fibers would remain at fiber surface,[34] and be detected by XPS and IR (Fig. 10 and Table II).

From the surface of separated CF (Table II), we can see that oxygen and nitrogen contents increase when compared with untreated CF. Beside small amount of sulfur element can be found on the surface of separated CF. The structure of the molecule adhesive on CF surface was characterized by IR spectrum (Fig. 10).

From Figure 10 we can see the peak at 1589 and 1487 cm^{-1} is the C=C stretching vibration of aromatic group; and a relatively stronger peak at 1666 cm^{-1} is due to the N—C=O vibration of bonded ketenes, the peak at 1241 cm^{-1} may be assigned to C—O stretching of ether. All peaks are critical peak of PPESK molecule.[35]

It can be seen that 5 min-plasma treatment time is sufferance to achieve chemical bonding interaction. While fiber surface roughness was changed a little. From Figure 8 we can see after plasma treated for 5 min composite ILSS is 71.3 MPa, ILSS is increased by 1.3 MPa, compared with that of the untreated CF/PPESK composite. However, after CF was treated for 15 min, fiber surface roughness has been increased significantly (Fig. 6). Composite ILSS is 79.0 MPa, composite interfacial adhesion was increased significantly. As can be seen from the analysis above, mechanical interaction has a dominant effect on composite interfacial adhesion than chemical bonding interaction.

CONCLUSION

Air plasma treatment was capable of increasing surface roughness as well as introducing surface polar groups onto CF; Surface modification is dominant at the beginning, and surface etching is dominant in the later stage; both chemical bonding and mechanical interaction were efficient in the enhancements of the ILSS of CF/PPESK composite; mechanical interaction has a dominant effect on composite interfacial adhesion than chemical bonding interaction.

This experiment is supported by National Defense 11th 5 year program Foundational Research Program No. A3520060215 and Liaoning Excellent Talents in University No. 2005RC-14.The authors acknowledge the valuable help given by the organizations. And acknowledgement also goes to our dear teachers Rongwen Lv for providing Dynamic Contact angle analysis system, Xinglin Li for XPS characterization, and Pro. Yudong Huang, Dr. Zaixing Jiang for AFM characterization.

Reference

1. Vlasveld, D. P. N.; Parlevliet, P. P.; Bersee, H. E. N. J Compos A: Appl Sci Manuf 2005, 36, 1.
2. Mitschang, P.; Blinzler, M.; Woginger, A. J Comp Sci Technol 2003, 63, 2099.
3. Rudolf, R.; Mitschang, P.; Neitzel, M. J Compos A 2000, 31, 1191.
4. Hou, M.; Ye, L.; Mai, Y.-W. J Plastics Rubber Compos Process Appl 1995, 23, 279.
5. Aiaz, J.; Rubio, L. J Mater Process Technol 2003, 143, 342.
6. He, J.; Wang, Y.; Zhang, H. J Compos Sci Technol 2000, 60, 1919.
7. Tang, L. G.; Kardos, J. L. J Polym Compos 1997, 18, 100.
8. Peng J.; Zhang, J.; Jan, X. Mater Rev 1999, 13, 482.
9. Yu Q.; Chen, P.; Lu, C. J Insul Mater 2005, 2, 50.
10. Montes-Moran, M. A.; Martinez-Alonso, A.; Tascon, J. M. D. J Carbon 2001, 39, 1057.
11. Bubert, H.; Ai, X.; Haiber, S. J Spectrochimica Acta B 2002, 57, 1601.
12. Dilsiz, N.; Ebert, E.; Weisweileer, W. J Colloid Interface Sci 1995, 170, 241.
13. Bismarck, A.; Emin Kumru, M.; Springer1, J. J Colloid Interface Sci 1999, 210, 60.
14. Dilsiz, N.; Ering, N. K.; Bayramli, E.; Akoval, G. J Carbon 1994, 33, 853.
15. Agostino, R. d.; Favia, P.; Oehr, C.; Wertheimer, M. R. Polymer 2005, 2, 7.
16. Lu, C.; Chen, P.; Yu, B. Adv Compos Lett 2007, 16, 33.
17. Jian, X.; Meng, Y.; Zheng, H.; Hay, A. S. China Pat. CN93109179.9 (1993).
18. Jian, X., Meng, Y.; Zheng, H.; Hay, A. S. China Pat. CN93109180.2 (1993).
19. Chen, P.; Yu, Q.; Lu, C.; et al. Am Chem Soc 2006, 231, 122.
20. Meng, Y. Z.; Hay, A. S.; Jian, X. G. J Appl Polym Sci 1997, 66, 1425.
21. Chen, P.; Lu, C.; Yu, Q. J Appl Polym Sci 2006, 102, 2544.
22. Chen P.; Lu, C.; Yu, Q. Chin J Mater Res 2005, 19, 159.

23. Park, J.-M.; Kim, D.-S.; Kim, S.-R. J Colloid Interface Sci 2003, 264, 431.
24. Park, J.-M.; Kim, D.-S.; Kong, J.-W. J Colloid Interface Sci 2002, 249, 62.
25. Luner, P. E.; Oh, E. J Colloids Surf A 2001, 181, 31.
26. Hoecker, F.; Karger-Kocsis, J. J Appl Polym Sci 1996, 59, 139.
27. Wu, G. M. J Mater Chem Phys 2004, 85, 81.
28. Lee, Y.-S.; Lee, B.-K. J Carbon 2002, 40, 2461.
29. Saïhi, D.; Ahmida, E.-A.; Abdellah, G. J Polym Testing 2002, 21, 615.
30. Zhao, Q.; Liu, Y.; Abel, E. W. J Colloid Interface Sci 2004, 280, 174.
31. Dilsiz, N.; Ebert, E.; Weisweiler, W.; Kovali, G. A. J Colloid Interface Sci 1995, 170, 241.
32. Jang, J.; Yang, H. J Mater Sci 2000, 35, 2297.
33. Morra, M.; Occhiello, E.; Garbassi, F. Surf Interface Anal 1990, 16, 412.
34. Weitzsacker, C. L.; Xie, M.; Drzal, L. T. Surf Interface Anal 1997, 25, 53.
35. Wang, J.-Y.; Liu, S.; Jian, X.-G. J Polym Mater Sci Eng 2002, 18, 49.